

Synthesis of Co-lean and Co-rich $\text{Li}_2\text{CoTi}_3\text{O}_8$ -based pigments: potential Co reduction and blue-green dichroism

Saho Kimura^a, Yoshikazu Suzuki^{a,b*}

^a Graduate School of Pure and Applied Sciences, University of Tsukuba, 1-1-1 Tennodai, Tsukuba, Ibaraki 305-8573, Japan

^b Faculty of Pure and Applied Sciences, University of Tsukuba, 1-1-1 Tennodai, Tsukuba, Ibaraki 305-8573, Japan

Abstract

$\text{Li}_2\text{CoTi}_3\text{O}_8$ pigment is a cobalt-based blue pigment and is highly safe as it is actually used for cosmetics such as an eye shadow and a lipstick. Despite its excellent features, available reports on $\text{Li}_2\text{CoTi}_3\text{O}_8$ blue pigment are quite limited. In this study, we demonstrate that the colors of CoO-lean compositions, cyanic blue, are substantially same as that of stoichiometric $\text{Li}_2\text{CoTi}_3\text{O}_8$, which contributes further reduction of Co resources. In addition, we also demonstrate that green color pigments can be synthesized just by increasing the CoO compositions. Li_2CO_3 , CoO and TiO_2 (anatase) powders were used as starting materials. The mixed powders were heat-treated at 1100 °C in air for 2 h to obtain $\text{Li}_2\text{CoTi}_3\text{O}_8$ powders, and they were characterized by X-ray diffraction, scanning electron microscopy, X-ray photoelectron spectroscopy and CIE1976- $L^*a^*b^*$ color coordinates measurement. Quantitative color measurement revealed that 10% reduction of CoO from stoichiometric $\text{Li}_2\text{CoTi}_3\text{O}_8$ is possible without much affecting the human eye feeling. Green colors appeared for the CoO-rich compositions, and the dichroism of the $\text{Li}_2\text{CoTi}_3\text{O}_8$ pigment was attributable to the valence change of Co ions from divalent (cyanic) to trivalent (greenish).

Key-words: A. Powders; solid state reaction; C: Color; D. Spinels; D. Transition metal oxides; Pigment; lithium cobalt titanate

* Corresponding author
E-mail: suzuki@ims.tsukuba.ac.jp
Faculty of Pure and Applied Sciences, University of Tsukuba,
1-1-1 Tennodai, Tsukuba, Ibaraki, 305-8573, Japan
Tel: +81-29-853-5026 / Fax: +81-29-853-4490

1. Introduction

Inorganic pigments are excellent in light fastness and durability, and are relatively inexpensive. They are widely applied to cosmetics and paints. There are many kinds of inorganic pigments, such as red iron oxide, white titanium oxide, cobalt blue and so on. Blue is one of the most common colors in the nature, but artificially creating the blue color has been considered difficult from a historical point of view. Currently, several synthetic blue pigments have been studied, such as cobalt blue (CoAl_2O_4) [1-3], lanthanum-strontium copper silicates ($\text{Sr}_{1-x}\text{La}_x\text{Cu}_{1-y}\text{Li}_y\text{Si}_4\text{O}_{10}$) [4], hibonite-based compounds, $A\text{Al}_{12-x}\text{M}_x\text{O}_{19}$ ($A = \text{Ca}, \text{Sr}$, or rare earths, $M = \text{Ni}$ etc.) [5], turquoise blue ($\text{Li}_{1.33}\text{Ti}_{1.66}\text{O}_4$) [6], calcium europium scandium silicate garnet ($(\text{Ca}_{1-x}\text{Eu}_x)_3\text{Sc}_2\text{Si}_3\text{O}_{12+\delta}$) [7], and lithium cobalt titanate ($\text{Li}_2\text{CoTi}_3\text{O}_8$) [8-11].

Amongst the synthetic blue pigments, we now focus on $\text{Li}_2\text{CoTi}_3\text{O}_8$. $\text{Li}_2\text{CoTi}_3\text{O}_8$ has a spinel-type crystal structure with a space group of $P4_332$, $a = 8.3766(12)$ Å (**Fig. 1**) [12-14]. Recently, $\text{Li}_2\text{CoTi}_3\text{O}_8$ is also studied as an anode material for lithium ion batteries due to its high specific lithium storage capacity and high electronic conductivity [14-16]. $\text{Li}_2\text{CoTi}_3\text{O}_8$ can be simply synthesized by a solid state method using Li_2CO_3 , CoO and TiO_2 .

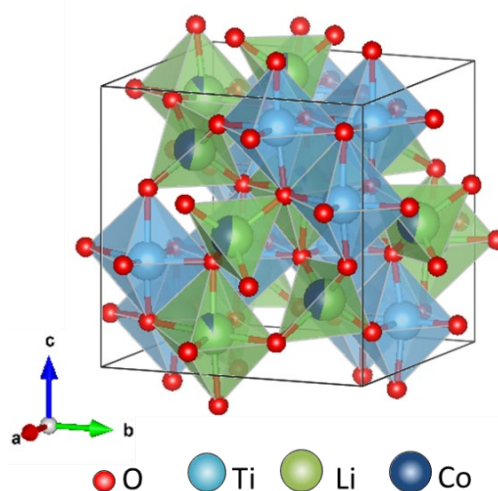


Fig. 1 Crystal structure of $\text{Li}_2\text{CoTi}_3\text{O}_8$ drawn with a reported data by Kawai et al [12].

$\text{Li}_2\text{CoTi}_3\text{O}_8$ pigment is a cobalt-based blue pigment and is highly safe as it is actually used for cosmetics such as an eye shadow and a lipstick. It is further excellent in acid resistance, alkali resistance, light resistance and heat resistance. Since it is excellent in dispersibility and stability, it is easy to mix with other pigments and it is possible to make a beautiful color tone. Despite these excellent features, available reports on $\text{Li}_2\text{CoTi}_3\text{O}_8$ blue pigment are quite limited. Nuss [8] synthesized $\text{Li}_2\text{CoTi}_3\text{O}_8$ -based spinel-type solid solutions for inorganic pigments. A. Kimura et al. [9] developed $\text{Li}_2\text{CoTi}_3\text{O}_8$ pigments coated on mica, which demonstrate blue and

green dichromatic luster. Costa de Carma et al. [10,11] reported the synthesis of nanosized $\text{Li}_2\text{CoTi}_3\text{O}_8$ particles, and studied the effect of synthetic temperatures on color.

As reported by A. Kimura et al., the greatest feature of the $\text{Li}_2\text{CoTi}_3\text{O}_8$ pigment is that it has high chroma and dichroism. Therefore, in this study, we have synthesized $\text{Li}_2\text{CoTi}_3\text{O}_8$ -based pigments with different CoO compositions, and studied the effect of CoO composition on color. Throughout this study, we demonstrate that the colors of CoO-lean compositions, cyanic blue, are substantially same as that of stoichiometric $\text{Li}_2\text{CoTi}_3\text{O}_8$, which contributes further reduction of Co resources. In addition, we also demonstrate that green color pigments can be synthesized just by increasing the CoO compositions.

2. Experimental

2.1 Synthesis of $\text{Li}_2\text{CoTi}_3\text{O}_8$ pigment powders

Li_2CO_3 ($\geq 99.0\%$, Wako Pure Chemical Industries, Ltd), CoO (90.0%, Wako) and TiO_2 (anatase) (99%, Kojundo Chemical Laboratory) powders were used as starting materials. To obtain stoichiometric $\text{Li}_2\text{CoTi}_3\text{O}_8$, these powders with the compositions of $\text{Li}_2\text{CO}_3:\text{CoO}:\text{TiO}_2 = 1:1:3$ (i.e., 20:20:60) in mol% were used. In order to study the effect of CoO composition, total 9 compositions with different CoO contents ($-20 \sim +20\%$) were examined (see Table 1). The Li_2CO_3 , CoO and TiO_2 (anatase) powders were weighed and mixed/pestled in an agate mortar for 10 min. The mixed powders in Al_2O_3 crucibles were heat-treated at $1100\text{ }^\circ\text{C}$ in air for 2 h. After the heat treatment, the synthesized $\text{Li}_2\text{CoTi}_3\text{O}_8$ powder aggregates were pestled in an agate mortar for 10 min to obtain $\text{Li}_2\text{CoTi}_3\text{O}_8$ pigment powders.

Table 1 Sample names and CoO compositions.

Sample name	CoO composition (mol%)	Normalized CoO molar ratio
C16.7	16.67	0.80
C17.5	17.53	0.85
C18.4	18.37	0.90
C19.2	19.19	0.95
C20	20.00	1.00
C20.8	20.79	1.05
C21.6	21.57	1.10
C22.3	22.33	1.15
C23.1	23.08	1.20

2.2 Characterization

The constituent phases of the $\text{Li}_2\text{CoTi}_3\text{O}_8$ powders were analyzed by X-ray diffraction (XRD, Multiflex, Cu-K α , 40 kV and 40 mA, Rigaku) at a scanning rate of 4°/min. The microstructure of the $\text{Li}_2\text{CoTi}_3\text{O}_8$ powders was observed by scanning electron microscopy (SEM, JSM-5600, JEOL). The valence numbers of cobalt ions in the $\text{Li}_2\text{CoTi}_3\text{O}_8$ powders were analyzed by X-ray photoelectron spectroscopy (XPS, JPS-9010TR, JEOL).

The color tones of the $\text{Li}_2\text{CoTi}_3\text{O}_8$ pigments were measured with a color reader (CR-20, Konica Minolta, Japan). CIE1976- $L^*a^*b^*$ color coordinates were evaluated. The $L^*a^*b^*$ color system is close to the human eye's feeling and is superior for comparing colors. L^* represents lightness, and combinations of two values of a^* and b^* express chroma and hue. The closer the value of L^* is to 100, the lighter the white color, the closer to 0 the darker the black color. Also, when the value of a^* is large in the positive direction, it becomes red, and when large in the negative direction, it becomes green. Also, when the value of b^* is large in the positive direction, it turns yellow and when large in the negative direction it becomes blue. In order to improve the reproducibility of the color measurement, each powder was uniaxially pressed into a pellet prior to the measurement. For each sample, $L^*a^*b^*$ values were determined as an average for 7 points. Chroma C^* , a color index for the colorfulness, is defined from the following equation including a^* and b^* , where high C^* means a clear and vivid color, while low C^* corresponds to a dark and dull color:

$$C^* = [(a^*)^2 + (b^*)^2]^{\frac{1}{2}}$$

Color difference ΔE^*_{ab} from the standard sample C20 is calculated from the following equation including ΔL^* , Δa^* and Δb^* :

$$\Delta E^*_{ab} = \sqrt{(\Delta L^*)^2 + (\Delta a^*)^2 + (\Delta b^*)^2}$$

Hue h , representing a color category, is calculated from the following equation including a^* and b^* , and it is plotted on a color circle:

$$h = \tan^{-1}\left(\frac{b^*}{a^*}\right)$$

3. Results and discussion

3.1 Sample appearance, crystal structure and microstructure

Figure 2 demonstrates appearances of the synthesized $\text{Li}_2\text{CoTi}_3\text{O}_8$ powders with different

CoO compositions. As is clearly seen from Fig. 2, the color became cyanic (azure-blue color) for CoO-lean and stoichiometric compositions, while it became greenish for CoO-rich compositions. These results are in good agreement with the literature by A. Kimura et al. on the dichromatic nature of $\text{Li}_2\text{CoTi}_3\text{O}_8$ [9].

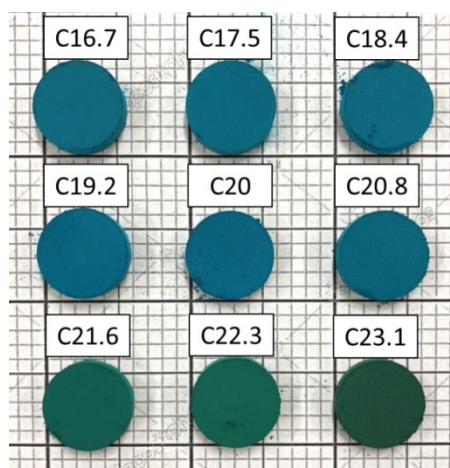


Fig. 2 Appearance of the synthesized $\text{Li}_2\text{CoTi}_3\text{O}_8$ powders with different CoO compositions (heat-treated at 1100 °C in air for 2 h, and uniaxially pelletized).

Figure 3 shows XRD patterns of the synthesized $\text{Li}_2\text{CoTi}_3\text{O}_8$ powders (measured without pelletizing). Five samples with stoichiometric and CoO-rich compositions, *i.e.*, C20, C20.8, C21.6, C22.3 and C23.1, were composed of single-phase $\text{Li}_2\text{CoTi}_3\text{O}_8$ spinel, while four samples with CoO-lean compositions, C16.7, C17.5, C18.4 and C19.2, were composed of $\text{Li}_2\text{CoTi}_3\text{O}_8$ spinel with a trace amount of TiO_2 rutile phase. Despite the existence of a trace TiO_2 rutile phase for the latter 4 samples, the appearance of 6 samples, C16.7, C17.5, C18.4, C19.2, C20 and C20.8, were quite similar to each other at least through our naked eyes (Fig. 2). This result strongly suggests the possibility of the CoO reduction for commercial $\text{Li}_2\text{CoTi}_3\text{O}_8$ -based pigments.

Figure 4 shows SEM micrographs of the synthesized $\text{Li}_2\text{CoTi}_3\text{O}_8$ powders (observed without pelletizing). All powders were composed of angular and equiaxed particles of $\sim 6 \mu\text{m}$. The microscale appearances of these powders are similar to each other. Note that the TiO_2 rutile particles for the C16.7-C19.2 samples cannot clearly be identified in this SEM observation. Throughout the SEM observation, it is suggested that the difference in colors (cyanic or greenish) cannot be attributed to the the particle morphology.

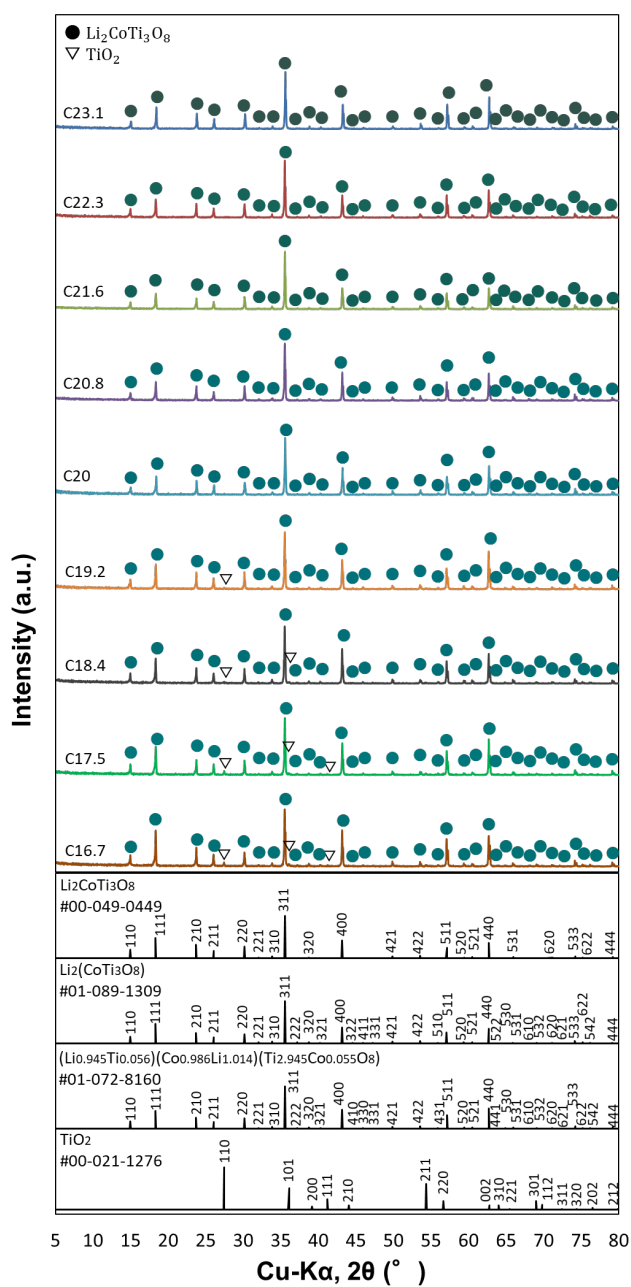


Fig. 3 XRD patterns of the synthesized $\text{Li}_2\text{CoTi}_3\text{O}_8$ powders (heat-treated at 1100 °C in air for 2 h). Reported XRD patterns for $\text{Li}_2\text{CoTi}_3\text{O}_8$ and TiO_2 rutile are also shown.

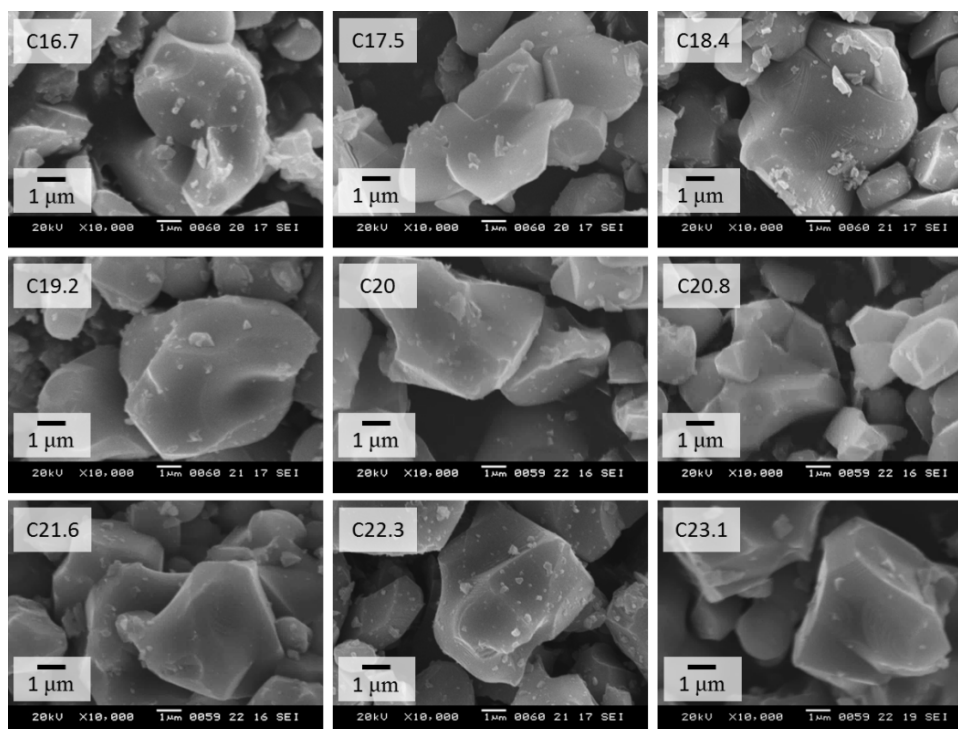


Fig. 4 SEM micrographs of the synthesized $\text{Li}_2\text{CoTi}_3\text{O}_8$ powders (heat-treated at $1100\text{ }^\circ\text{C}$ in air for 2 h).

3.2 Color characterization

Figure 5 represents the results of color measurement. Each sample had a color close to blue or green because the values of a^* and b^* are both negative. The L^* , a^* and b^* values of the 6 samples of CoO-lean C16.7, C17.5, C18.4, C19.2 and near-stoichiometric C20, C20.8 were similar to each other, which is in good agreement with the naked-eye observation (see Fig. 2). However, there exists significant differences of $L^*a^*b^*$ values between C20.8 and C21.6. Therefore, in order to compare the colors in more detail, chroma, color difference and hue angle were calculated from the results of this color measurement.

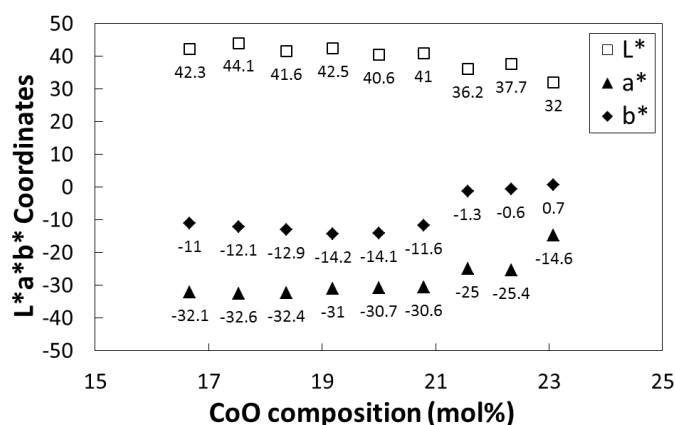


Fig. 5 CIE- $L^*a^*b^*$ color coordinates of the synthesized $\text{Li}_2\text{CoTi}_3\text{O}_8$ powders with different CoO compositions (heat-treated at 1100 °C in air for 2 h, and uniaxially pelletized as shown in Fig. 2).

Figure 6 shows the relationship between CoO composition and chroma. The larger the chroma value is, the brighter the color is, and the smaller the chroma value, the dull the color. Chroma decreased with increasing CoO compositions, particularly for the CoO-rich samples of C21.6, C22.3 and C 23.1.

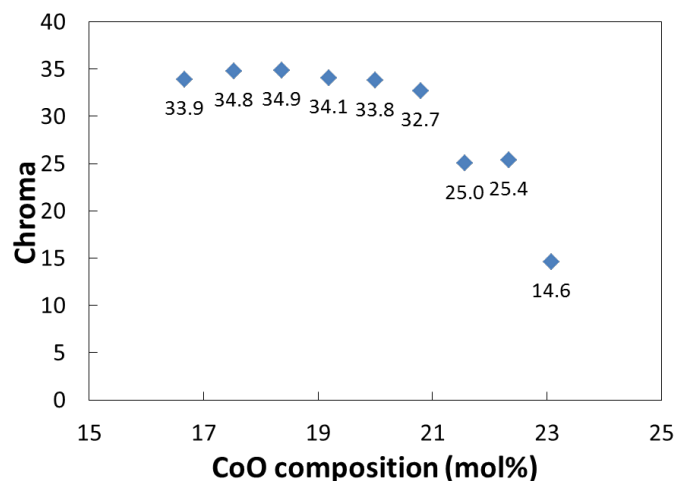


Fig. 6 Chroma C^* of the synthesized $\text{Li}_2\text{CoTi}_3\text{O}_8$ powders with different CoO compositions (heat-treated at 1100 °C in air for 2 h, and uniaxially pelletized as shown in Fig. 2).

Table 2 summarizes the color difference ΔE^*_{ab} from the C20 reference. **Table 3** also shows the relationship between color difference and human eyes feeling, reported by Konica

Minolta Co. [17]. In general, when the color difference is 3.0 or less, two colors are recognized as same via human eye observation, and when it is 12.0 or more, two colors are recognized as different. From Tables 2 and 3, ΔE^*_{ab} for the CoO-lean samples of C19.2 and C18.9 are less than 3.0, which means that 10% reduction of CoO (*i.e.*, C18.4) is possible without much affecting human eye feeling. Also from Tables 2 and 3, the colors of the CoO-rich samples of C21.6, C22.3, C23.1 are clearly different from that of C20, because ΔE^*_{ab} was more than 12.0. That is reasonable with staring into Fig. 2.

Table 2 Color difference (ΔE^*_{ab}) from C20.

Sample name	Color difference (ΔE^*_{ab}) with C20
C16.7	3.80
C17.5	4.46
C18.4	2.31
C19.2	1.93
C20	–
C20.8	2.53
C21.6	14.69
C22.3	14.79
C23.1	23.50

Table 3 Correlation between color difference ΔE^*_{ab} and human eye feeling*.

Color difference (ΔE^*_{ab})	Human eye feeling
~0.1	Human cannot discriminate a color difference visually.
0.1~0.2	The lower limit of the color difference that enables a skilled professional to discriminate between different colors.
0.2~0.4	The lower limit of the color difference that enables an ordinary person to discriminate between different colors.
0.4~0.8	Upper limit of the color difference used for butting parts etc. where strict color management is required.
0.8~1.5	Upper limit of color difference used in product color management.
1.5~3.0	A color difference range generally regarded as the same color, without noticing a different color if products are separated and arranged.
3.0~	Complaints due to different colors can occur.
12.0~	When there is a color difference above this value, it is regarded as a different color tone.

*Partially modified from the Konica Minolta Technical Document 2018 (in Jpn.) [17].

Figure 7 shows hue angles of the synthesized $\text{Li}_2\text{CoTi}_3\text{O}_8$ powders with different CoO compositions displayed on a 2-D simplified $L^*a^*b^*$ color space diagram cut in the horizontal direction. The CoO-lean and near-stoichiometric 6 samples (C16.7, C17.5, C18.4, C19.2, C20, C20.8) belong to the cyan tone, while the CoO-rich 3 samples (C21.6, C22.3, C23.1) belong to the green tone.

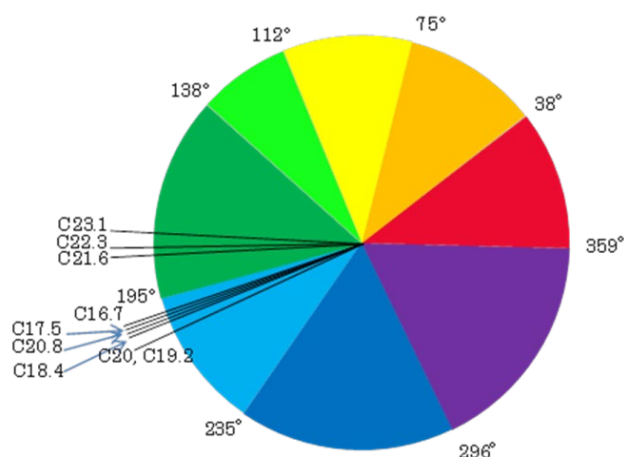


Fig. 7 Hue angle h of the synthesized $\text{Li}_2\text{CoTi}_3\text{O}_8$ powders with different CoO compositions (heat-treated at 1100 °C in air for 2 h, and uniaxially pelletized as shown in Fig. 2), displayed on a 2-D simplified $L^*a^*b^*$ color space diagram cut in the horizontal direction. Dichromatic color nature, *i.e.*, cyan and green, was confirmed.

3.3 Valence number of Co ions

In order to investigate the origin of the color difference, the electronic state was examined by XPS measurement. **Figure 8** shows an XPS analysis for Co 2p_{3/2} performed on the selected five samples, *viz.*, C16.7, C18.4 and C20 with cyan tone, and C21.6 and C23.1 with green tone. In these figures, black, yellow, blue, green and red lines indicates the measured value, divalent Co^{2+} , trivalent Co^{3+} , satellite, and the sum of blue, yellow and green lines, respectively. Peak intensity of the divalent Co^{2+} (yellow line) was relatively high for the cyanic colored samples, whereas that of the trivalent Co^{3+} (blue line) was much high for the green colored C21.6 and C23.1. The XPS analysis suggests that the excess of CoO in the starting mixture increased the Co^{3+} portion in the final product.

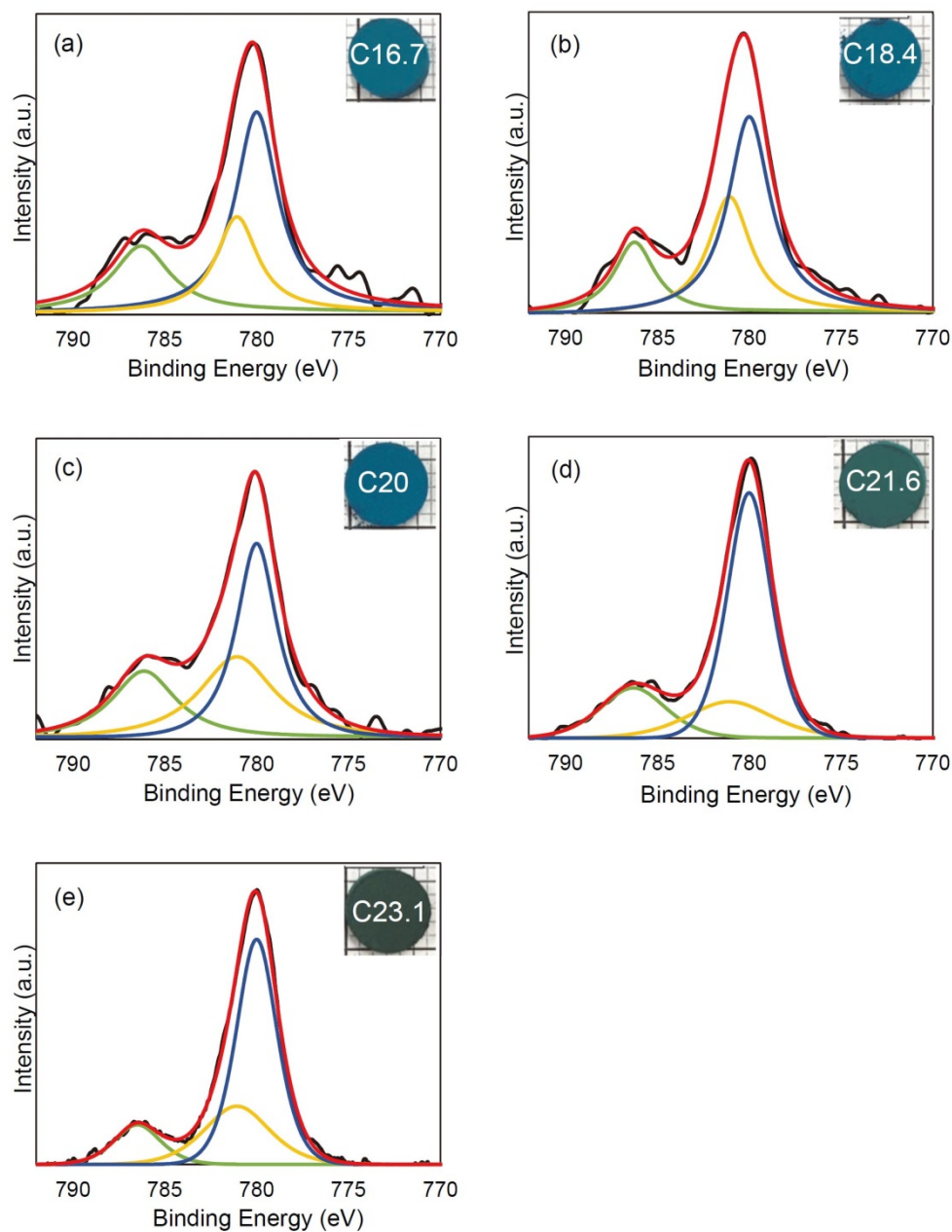


Fig. 8 Co 2p_{3/2} X-ray photoelectron spectra for five selected Li₂CoTi₃O₈ powders (heat-treated at 1100 °C in air for 2 h): (a) C16.7, (b) C18.4, (c) C20, (d) C21.6 and (e) C23.1. Black, yellow (781.075 eV), blue (780.001 eV), green and red lines indicates the measured value, divalent Co²⁺, trivalent Co³⁺, satellite, and the sum of yellow, blue and green lines, respectively. Note that the green line will be further deconvoluted into Co²⁺ and Co³⁺ satellite peaks for a quantitative analysis

A. Kimura et al. [9] considered that the origin of the dichroism of the $\text{Li}_2\text{CoTi}_3\text{O}_8$ pigment is the result of a slight lattice parameter difference that affected crystal lattice vibration and changed energy absorption. However, the differences in lattice constants were very small. Considering the XPS results in this study, the origin of the dichroism of the $\text{Li}_2\text{CoTi}_3\text{O}_8$ pigment is rather attributable to the valence change of Co ions from divalent (cyanic) to trivalent (greenish).

4. Conclusions

In this study, we have synthesized $\text{Li}_2\text{CoTi}_3\text{O}_8$ -based pigments with different CoO compositions, and studied the effect of CoO composition on color. In conclusions:

- (1) XRD revealed that five samples with stoichiometric and CoO-rich compositions, *i.e.*, C20, C20.8 (+5%), C21.6 (+10%), C22.3 (+15%) and C23.1 (+20%), were composed of single-phase $\text{Li}_2\text{CoTi}_3\text{O}_8$ spinel, while four samples with CoO-lean compositions, C16.7 (-20%), C17.5 (-15%), C18.4 (-10%) and C19.2 (-5%), were composed of $\text{Li}_2\text{CoTi}_3\text{O}_8$ spinel with a trace amount of TiO_2 rutile phase.
- (2) The color difference ΔE^*_{ab} for the CoO-lean samples of C19.2 and C18.4 are less than 3.0, which means that 10% reduction of CoO in $\text{Li}_2\text{CoTi}_3\text{O}_8$ (*i.e.*, C18.4) is possible without much affecting human eye feeling.
- (3) Green colors appeared for the CoO-rich compositions, and the dichroism of the $\text{Li}_2\text{CoTi}_3\text{O}_8$ pigment is rather attributable to the valence change of Co ions from divalent (cyanic) to trivalent (greenish).

Acknowledgment

We thank the Open Facility Network Office, Research Facility Center for Science and Technology, University of Tsukuba, for the SEM observation and the XPS measurement. We also thank Dr. Momma and Dr. Izumi for offering a crystal drawing free software VESTA Ver. 3 [18].

References

- [1] M. Bouchard, A. Gambardella, Raman microscopy study of synthetic cobalt blue spinels used in the field of art, *J. Raman. Spectro.* 41 (2010) 1477-1485.
- [2] M. Yoneda, I. Gotoh, M. Nakanishi, T. Fujii, T. Nomura, Influence of aluminum source on the color tone of cobalt blue pigment, *Powd. Tech.* 323 (2018) 574-580.
- [3] A. A. Ali, E. El Fadaly, I. S. Ahmed, Near-infrared reflecting blue inorganic

- nano-pigment based on cobalt aluminate spinel via combustion synthesis method, *Dyes Pigments*. 158 (2018) 451-462.
- [4] S. Jose, M. L. Reddy, Lanthanum-strontium copper silicates as intense blue inorganic pigments with high near-infrared reflectance, *Dyes Pigments*. 98 (2013) 540-546.
- [5] J. Li, E. A. Medina, J. K. Stalick, A. W. Sleight, M. A. Subramanian, Colored oxides with hibonite structure: A potential route to non-cobalt blue pigments, *Prog. Solid State Chem.* 44 (2016) 107-122.
- [6] A. Fernández-Osorio, M. P. Jiménez-Segura, A. Vázquez-Olmos, R. Sato-Berru, Turquoise blue nanocrystalline pigment based on $\text{Li}_{1.33}\text{Ti}_{1.66}\text{O}_4$: Synthesis and characterization, *Ceram. Int.*, 37 (2011) 1465-1471.
- [7] Wendusu, T. Honda, T. Masui, N. Imanaka, Novel environmentally friendly inorganic blue pigments based on calcium scandium silicate garnet, *Chem. Lett.* 42 (2013) 1562-1564. (* no initial for Wendusu)
- [8] J. W. Nuss, Inorganic pigment comprising a solid solution of differing spinels, US Patent No. 4075029 (1978).
- [9] A. Kimura, Y. Ikuta and F. Suzuki, Development of high chroma and dichromatic luster pigments by synthesis of $\text{Li}_2\text{CoTi}_3\text{O}_8$ onto the surface of mica, *Shikizai (in Jpn.)*. 69 (1996) 810-818.
- [10] M. S. C. da Camara, L. A. Pimentel, E. Longo, L. de Nobrega Azevedo, D. M. de Araujo Melo, Spinel $\text{Li}_2\text{CoTi}_3\text{O}_8$ nanometer obtained for application as pigment, *Bol. Soc. Esp. Ceram. V. (in Esp.)* 55 (2016) 71-78.
- [11] M. S. C. da Camara, Synthesis and characterization at the nanometer level of the $\text{Li}_2(\text{M})\text{Ti}_3\text{O}_8$ phase, M = Zn, Co and Ni hair Pechini method, Ph. D. thesis, Federal University of São Carlos, Brazil, 2004.
- [12] H. Kawai, M. Tabuchi, M. Nagata, H. Tukamoto, A. R. West, Crystal chemistry and physical properties of complex lithium spinels $\text{Li}_2\text{MM}'_3\text{O}_8$ (M=Mg, Co, Ni, Zn; M'=Ti, Ge), *J. Mater. Chem.* 8 (1998) 1273-1280.
- [13] N. Reeves, D. Pasero, A. R. West, Order-disorder transition in the complex lithium spinel $\text{Li}_2\text{CoTi}_3\text{O}_8$, *J. Solid State Chem.* (2007) 1894-1901.
- [14] W. Chen, R. Du, W. Ren, H. Liang, B. Xu, J. Shu, Z. Wang, Solid state synthesis of $\text{Li}_2\text{Co}_{0.5}\text{Cu}_{0.5}\text{Ti}_3\text{O}_8$ and $\text{Li}_2\text{CoTi}_3\text{O}_8$ and their comparative lithium storage properties,

Ceram. Int. 40 (2018) 13757-13761.

- [15] L. Wang, Q. Z. Xiao, Z. H. Li, G. T. Lei, L. J. Wu, P. Zhang, J. Mao, Synthesis of $\text{Li}_2\text{CoTi}_3\text{O}_8$ fibers and their application to lithium-ion batteries, *Electrochim. Acta*, 77 (2012) 77-82.
- [16] J. Wang, H. Zhao, Y. Shen, Z. Du, X. Chen, Q. Xia, Structure, stoichiometry, and electrochemical performance of $\text{Li}_2\text{CoTi}_3\text{O}_8$ as an anode material for lithium-ion batteries, *ChemPulsChem*, 78 (2013) 1530-1535.
- [17] Konica Minolta Co., Ltd., Konica Minolta Color Measurement Seminar Material Ver. 2018 (in Jpn.).
- [18] K. Momma and F. Izumi, VESTA 3 for three-dimensional visualization of crystal, *J. Appl. Crystallogr.*, 44 (2011) 1272-1276.